JOURNAL OF CHEMICAL INFORMATION AND MODELING

ARTICLE

pubs.acs.org/jcim

A Mechanistic Hypothesis for the Cytochrome P450-Catalyzed Cis−Trans Isomerization of 4-Hydroxytamoxifen: An Unusual Redox Reaction

Li Gao,[†,⊥] Yaoquan Tu,[†,⊥] Pia Wegman,[‡] Sten Wingren,[‡] and Leif A. Eriksson*[,§,∥]

[†]Örebro Life Science Center, School of Science and Technology, Örebro University, 70182 Örebro, Sweden

[‡]Department of Health and Medical Sciences, Örebro University, 70182 Örebro, Sweden

[§]School of Chemistry, National University of Ireland - Galway, Ireland

Supporting Information

ABSTRACT: We provide a detailed description of the cis−trans isomerization of 4-hydroxytamoxifen/endoxifen catalyzed by several isoforms from the cytochrome P450 (CYP) superfamily, including CYP1B1, CYP2B6, and CYP2C19. We show that the reactions mainly involve redox processes catalyzed by CYP. DFT calculation results strongly suggest that the isomerization occurs via a cationic intermediate. The cationic cis-isomer is more than 3 kcal/mol more stable than the trans form, resulting in an easier conversion from trans-to-cis than cis-to-trans. The cis−trans isomerization is a rarely reported CYP reaction and is ascribed to the lack of a second abstractable proton on the ethenyl group of the triarylvinyl class of substrates. The cationic intermediates thus formed instead of the stable dehydrogenation products allow for isomerization to occur. As a comparison, the reactions for the tamoxifen derivatives are compared to those of other substrates, 4-hydroxyacetanilide and raloxifene, for which the stable dehydrogenation products are formed.

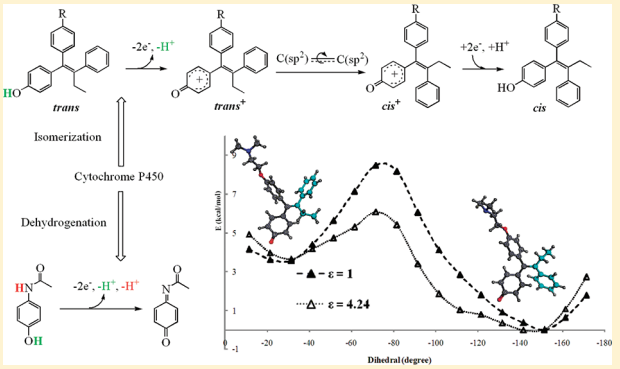

1. INTRODUCTION

Breast cancer is the leading type of cancer in women worldwide. The antiestrogen tamoxifen (TAM) has been widely used for the endocrine treatment of all stages of estrogen receptor (ER) positive breast cancer.[1] TAM undergoes extensive hepatic metabolism whereby it is predominantly metabolized by human CYP enzymes to the corresponding *N*-desmethyl, 4-hydroxy, and α-hydroxy metabolites. This biotransformation of TAM is important in converting the parent compound to the active or toxic metabolites.[2−4] The 4-hydroxy metabolites shown in Scheme 1, including 4-hydroxy-TAM (OHT) and 4-hydroxy-*N*-desmethyl-TAM (endoxifen/ENDO), exhibit a high affinity to ERα, resulting in 30- to 100-fold more potency than the parent drug TAM.[5−7]

Chemically, TAM is a trans form of a triarylvinyl class of compounds, which exist in both the solid state and solution in a chiral propeller conformation where the aryl groups are all twisted in the same sense, radiating from the alkene bond.[8,9] X-ray studies showed that crystalline TAM is a 'counterclockwise' molecular propeller,[10] whereas OHT exists as a 'clockwise' propeller when cocrystallized with ERα (PDB Code: 3ERT, 2JF9, and 2BJ4).[11−13] The propeller conformations represent low-energy conformers from a compromise between conjugation and steric effects.[14,15] The interconversion between the vinyl propellers differing in helicity occurs through internal rotation around the C(Ar)−C(sp^2) bonds. Dynamic NMR detection has shown that TAM undergoes a rapid helicity reversion at room temperature as well as at −75 °C,[16] which indicates a low rotational barrier for the C(Ar)−C(sp^2) single bonds. In contrast, rotation around the C(sp^2)=C(sp^2) double bond is energetically expensive and results in the cis−trans isomerization of TAM derivatives.

cis-4-Hydroxytamoxifen (*cis*-OHT) has, besides *trans*-OHT, been detected in breast tumors of patients treated by *trans*-TAM. Although *trans*-OHT is a potent antiestrogen with much higher affinity to the estrogen receptor compared to TAM, it hence also isomerizes to the less potent cis isomer.[17,18] The cis−trans isomerization does not occur for TAM itself. The relatively high *cis*:*trans*-OHT ratio has been associated with clinical resistance to tamoxifen therapy, which has triggered a great interest in trying to understand the cis−trans isomerization processes.[19,20] Experimental data is limited for the other 4-hydroxy metabolite ENDO (Scheme 1), for which the trans isomers has as potent antiestrogenic effects as *trans*-OHT in breast cancer cells and displays much higher plasma concentration in vivo.[6] While the existence of *cis*-ENDO in breast tumors and the cis−trans isomerization

Received: March 4, 2011
Published: August 28, 2011

Scheme 1. TAM and Its Important Metabolites

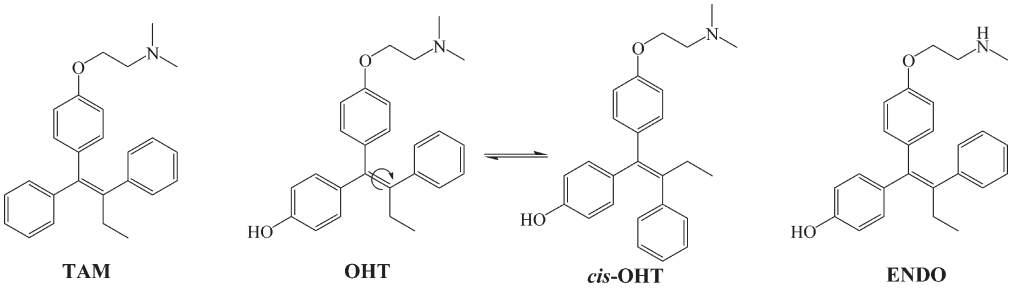

Scheme 2. A. Possible Pathways for the Trans-to-Cis Isomerization of OHT/ENDO Catalyzed by CYP. B. Resonance Isomerism of the Radical and Cationic Intermediates[a]

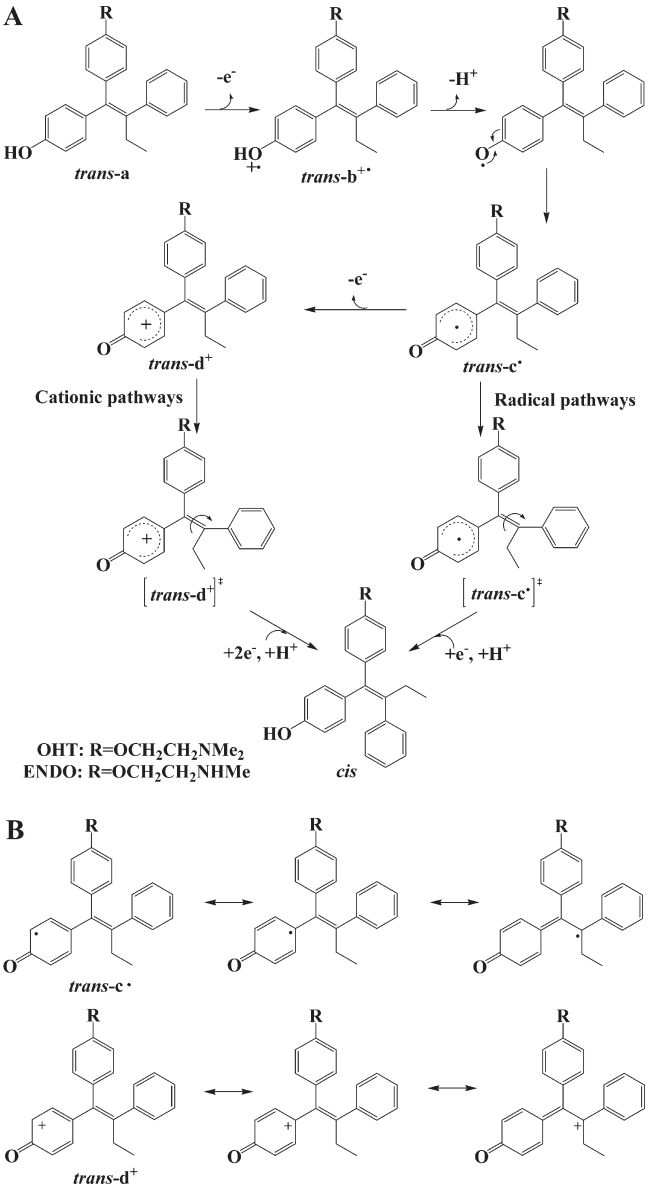

[a] It is argued that the cis-to-trans reaction proceeds by analogous mechanisms, via the *cis*-$\mathbf{c}^{\bullet}$ or *cis*-$\mathbf{d}^{+}$ intermediates.

reaction have not been investigated experimentally, it is also in this case known to be less potent than the trans form.[21]

The cis−trans interconversion of OHT is mediated by CYP enzymes, including human liver microsomes[22] and recombinant human CYPs. It is principally catalyzed by CYP1B1, with CYP2B6 and CYP2C19 also contributing.[23] The heme-containing CYP enzymes play a critical role for the metabolism of numerous physiologically important endogenous and exogenous substrates and catalyze diverse types of reactions including hydroxylation, epoxidation, dehydrogenation, and heteroatom oxidation.[24,25] Extensive research has been performed on the chemically versatile CYP isoform superfamily. A branch thereof is theoretical studies, which aims to understand the fast and efficient oxidation reactions under physiological conditions.[26−31] The consensus active species of heme-containing CYPs is the high-valent iron-oxo porphyrin species, Compound I (Cpd I), with electrophilic attacking character.

As a result, CYP-mediated reactions stem from the same type of oxidation mechanism and involve initial steps that can be viewed as an electrophilic attack on the substrate. The usual initial steps can include the iron-oxo species abstraction of an H atom or an electron from the substrate, or attack on the π system of a substrate aromatic ring.[27,32,33] The resulting intermediates may be subsequently partitioned according to differential possible pathways. For instance, the consensus mechanism of aliphatic hydroxylation proceeds via an initial H atom abstraction followed by OH rebound.[34,35] In the dehydrogenation route, on the other hand, after the initial H atom abstraction, the radical intermediate loses one more H atom (mostly like a sequential loss of electron and proton), resulting in the olefin product.[36,37] For amine N-dealkylation, electron abstraction from the N atom is generally accepted as the initial step, followed by proton transfer from the N-radical cation and subsequent bond rupture.[38] Moreover, for aromatic hydroxylation, a more efficient mechanism, compared to H abstraction followed by OH rebound, was proposed to start from electrophilic attack of the π system of the aromatic ring, leading to a Fe−O−Ph intermediate, followed by a proton-shuttle.[39]

For the CYP-mediated cis−trans isomerization of OHT, there is no change in the oxidation−reduction state, although the requirement for NADPH as cofactor[22,23] argues that a redox process should be involved. Besides the consensus mechanism initiated by Cpd I, Cpd 0 has recently also been shown to be involved in the CYP oxidation process.[40] The cis−trans isomerization is not a commonly reported CYP reaction, and a detailed understanding of the mechanism is still lacking. In the present work, we focus on a theoretical exploration of the *substrates* to reveal the CYP reaction mechanisms, not including in our model

Scheme 3. A. Structures and Ring Labeling of *trans*- and *cis*-OHT/ENDO. B. Possible Mechanisms for the Trans/Cis-Isomerization of OHT/ENDO through the Cationic Intermediate as a Process in Conjunction with the Rotation around the C(Ar)−C(sp^2) Bond, Which Results in Helicity Reversion

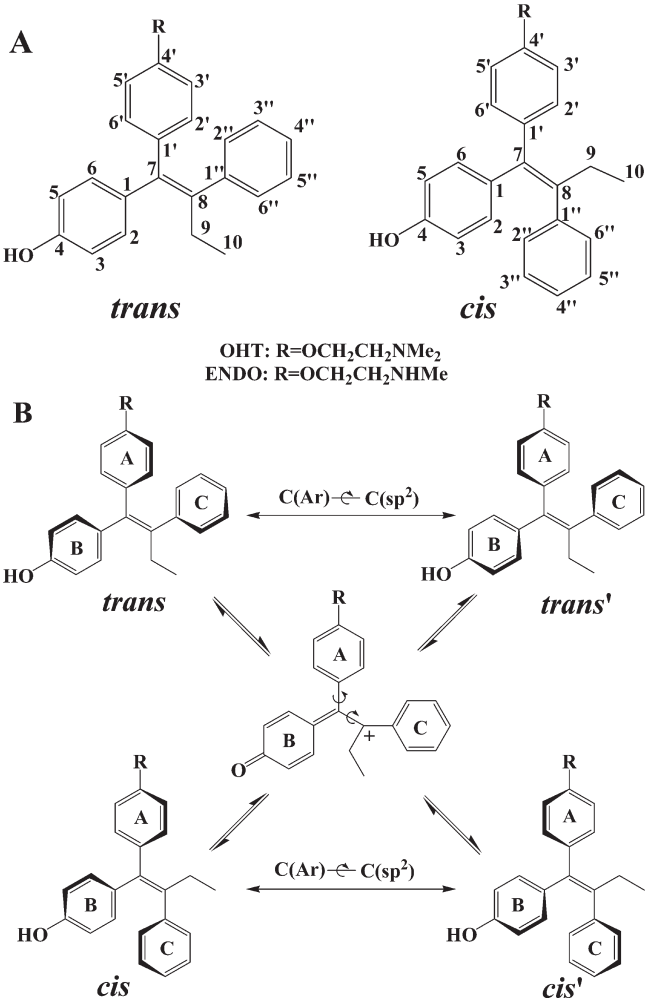

the complex mechanistic pictures of the explicit heme-containing oxidation steps. Two possible mechanisms are compared by qualitatively evaluating the activation energies. The computed

Table 2. Energy Barriers ($\Delta\Delta G^{\ddagger}$, in kcal/mol) of the Rotation about the Double Bond for Trans-to-Cis and Cis-to-Trans Isomerization via Radical and Cationic Intermediates[a]

	OHT		ENDO	
reaction	$\varepsilon = 1$	$\varepsilon = 4.24$	$\varepsilon = 1$	$\varepsilon = 4.24$
trans → cis [*trans*-**c**$^{\bullet}$]‡	17.3	15.1	15.9	15.2
cis → trans [*cis*-**c**$^{\bullet}$]‡	17.1	17.1	18.0	16.8
trans → cis [*trans*-**d**$^{+}$]‡	5.0	1.8	4.9	2.3
cis → trans [*cis*-**d**$^{+}$]‡	10.8	7.7	10.4	7.8
experimental[b]	51−64%/trans → cis			
	22−27%/cis → trans			

[a] All values are relative to the free energies of the corresponding reaction intermediates. [b] CYP-catalyzed isomerization of OHT was carried out by incubating pure *trans*- or *cis*-OHT with human liver microsomes for 40 min in the presence of an NADPH-generating system.[22]

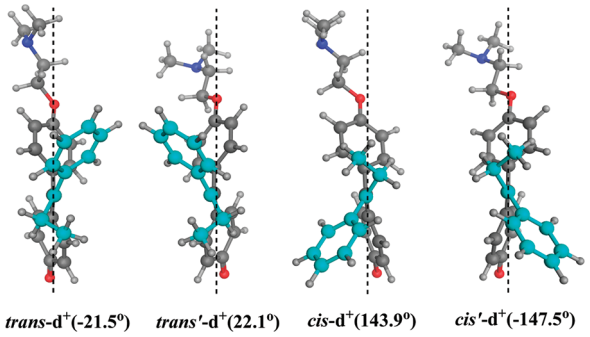

Figure 1. Optimized structures of the cationic intermediates for *trans*/*cis*-OHT in the gas phase. The carbon atoms of benzene and ethyl substituents are colored cyan, which are highly twisted from the plane of the double bond and assumed to rotate around the double bond. The dihedral angles of 1′−7−8−1″ labeled in Scheme 3A are measured from the optimized structures.

Table 1. ZPE Corrected Electronic Energies and Selected Geometrical Parameters for Different Species of OHT Optimized in the Gas Phase

		bond length (Å)					dihedral (deg)
system	ΔE (kcal/mol)	C4−O4	C1−C7	C7−C8	C7−C1′	C8−C1″	1′−7−8−1″
trans-**a**	0.0	1.363	1.494	1.355	1.493	1.494	−9.8
trans′-**a**	−0.1	1.364	1.492	1.355	1.493	1.493	9.5
trans-**c**$^{\bullet}$	396.6	1.246	1.475	1.363	1.494	1.492	−10.4
trans′-**c**$^{\bullet}$	396.3	1.246	1.475	1.362	1.494	1.491	10.1
trans-**d**$^{+}$	560.0	1.216	1.414	1.424	1.485	1.450	−21.5
trans′-**d**$^{+}$	559.4	1.216	1.413	1.425	1.485	1.450	22.1
cis-**a**	0.0	1.364	1.493	1.354	1.492	1.493	172.1
cis′-**a**	0.0	1.364	1.493	1.354	1.493	1.493	−171.6
cis-**c**$^{\bullet}$	395.5	1.245	1.477	1.362	1.493	1.489	169.7
cis′-**c**$^{\bullet}$	395.8	1.245	1.476	1.363	1.493	1.489	−169.4
cis-**d**$^{+}$	556.9	1.216	1.405	1.430	1.484	1.440	143.9
cis′-**d**$^{+}$	556.5	1.216	1.408	1.428	1.483	1.442	−147.5

dx.doi.org/10.1021/ci2001082 |*J. Chem. Inf. Model.* 2011, 51, 2293–2301

Table 3. Total Gibbs Free Energies and Selected Geometrical Parameters for Cationic Transition States of OHT Optimized in Gas Phase

		bond length (Å)					dihedral (deg)
system	ΔG (a.u.)	C4−O4	C1−C7	C7−C8	C7−C1′	C8−C1″	1′−7−8−1″
[*trans*-**c**$^{\bullet}$]‡	−1211.850351	1.224	1.365	1.487	1.495	1.434	−100.3
[*cis*-**c**$^{\bullet}$]‡	−1211.852600	1.224	1.367	1.490	1.487	1.435	96.3
[*trans*-**d**$^{+}$]‡	−1211.608370	1.217	1.364	1.480	1.481	1.418	−73.2
[*cis*-**d**$^{+}$]‡	−1211.605152	1.216	1.359	1.486	1.489	1.417	83.6

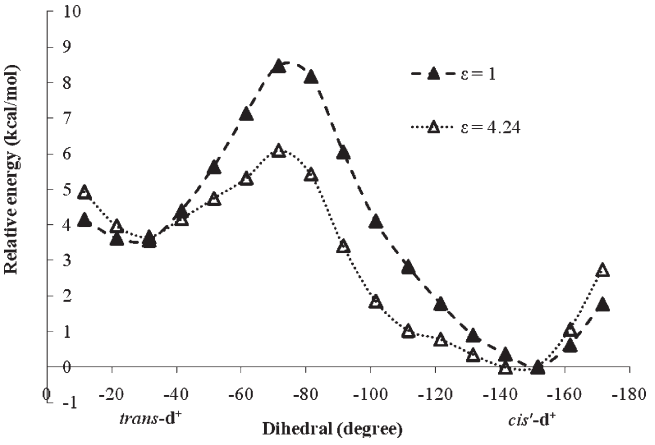

Figure 2. Computed energy profiles of cis−trans isomerization of OHT via the cationic intermediate. Pure DFT energies (ε = 1 and ε = 4.24) obtained at the M06-2X/6-31+G(d,p) level of theory with ZPE correction.

activation energies indicate that a similar isomerization process can occur also for ENDO.

2. COMPUTATIONAL METHODS

The hybrid meta-GGA exchange-correlation functional M06-2X[41,42] in conjunction with the 6-31+G(d,p) basis set was used for all calculations except for raloxifene which was studied using the M06−2X/6-31G(d,p) level of theory. Geometry optimizations were carried out both in vacuo and modeling the bulk effect of a protein environment (ε = 4.24) for all species including the different transition states. Starting geometries were built according to the crystalline tamoxifen structure.[10] Harmonic vibrational frequency calculations were performed following the geometry optimizations at the same level of theory, to analyze the nature of stationary structures on the potential energy surface and to extract thermal corrections to the Gibbs free energies at 298 K. The hydrophobic environment of the CYP active site was considered using the SMD continuum solvation model.[43] All calculations were performed using the Gaussian 09 program package.[44]

3. RESULTS AND DISCUSSION

3.1. Possible Pathways. The mechanistic studies on the CYP-catalyzed cis−trans isomerization start from the rotation about the C(sp^2)=C(sp^2) double bond, which is energetically expensive in simple systems. Two possible pathways were investigated, which differ with regard to the rotational intermediates as depicted in Scheme 2. CYP-catalyzed oxidation on OHT/ENDO give radical or cationic intermediates in which the alkene bond is disrupted, as shown in the resonance isomerism (Scheme 2B), and enables the isomerization to occur.

The isomerization arises from an initial (net) hydrogen abstraction from the 4-OH substituent. This is supported by experimental data, in that no isomerization is detected for TAM itself. It is also consistent with the generally accepted mechanism for many CYP-catalyzed reactions,[26,33] with initial H-atom abstraction from the substrate leading to putative radical intermediates. Williams et al. carried out experimental studies of the cis−trans isomerization of OHT catalyzed by human CYPs, and proposed a subsequent rotation about the alkene bond via the radical intermediate.[22] However, the high-valent ferryl species of the heme complex may further oxidize the substrate to a cationic intermediate followed by the isomerization step, as proposed in this work.

3.2. Geometry. An important characteristic for the triarylvinyl class of compounds is the vinyl propeller structure as shown in Scheme 3, in which the three rings twist in a correlated rotation, resulting in a 'clockwise' (trans′-/cis′-isomer in Scheme 3B) or 'counterclockwise' (trans-/cis-isomer in Scheme 3B) molecular propeller. The interconversion between the different helicities takes place through internal rotation around the C(Ar)−C(sp^2) bonds, which is a rapid and low energy cost process for TAM as detected by experiments.[16] The energy difference between opposite helicity is for each species about 0−0.6 kcal/mol as shown in Table 1.

For the case of rotation via the cationic intermediate, the optimized structures are shown in Figure 1 for the trans and cis forms with opposite helicity. The possible rotation processes through the cationic intermediate are depicted in Scheme 3B. The rotation process from *trans*-**d**$^{+}$ to *cis*′-**d**$^{+}$ crosses the radian of 126° as the dihedral angle 1′−7−8−1″ changes from −21.5° to −147.5°, while the isomerization from *trans*-**d**$^{+}$ to *cis*-**d**$^{+}$ crosses the radian of more than 160° as the dihedral angle 1′−7−8−1″ changes from −21.5° to 143.9°. Therefore, the trans↔cis′ isomerization process is more efficient than the trans↔cis process, which retains the same helicity. We thus propose a helicity reversion in conjunction with cis−trans isomerization, i.e., the isomerization process of trans↔cis′ or trans′↔cis.

The resonance effects on the double bond caused by the radical or cationic intermediates are seen from the geometrical changes displayed in Table 1. For the radical intermediates (*trans*-/*cis*-**c**$^{\bullet}$), the C4−O4 bond length decreases from 1.36 Å to 1.25 Å and with only slight changes in C1−C7 and C7−C8 bond length, which indicates the resonance isomerism between the phenol radical and quinone with necessary rearrangement of double bonds. Similar but more pronounced changes are found

Scheme 4. The Major CYP Isoforms for 4-Hydroxylation and α-Hydroxylation of TAM and Possible Initial H Atom Abstraction (R = $OCH_2CH_2NMe_2$)

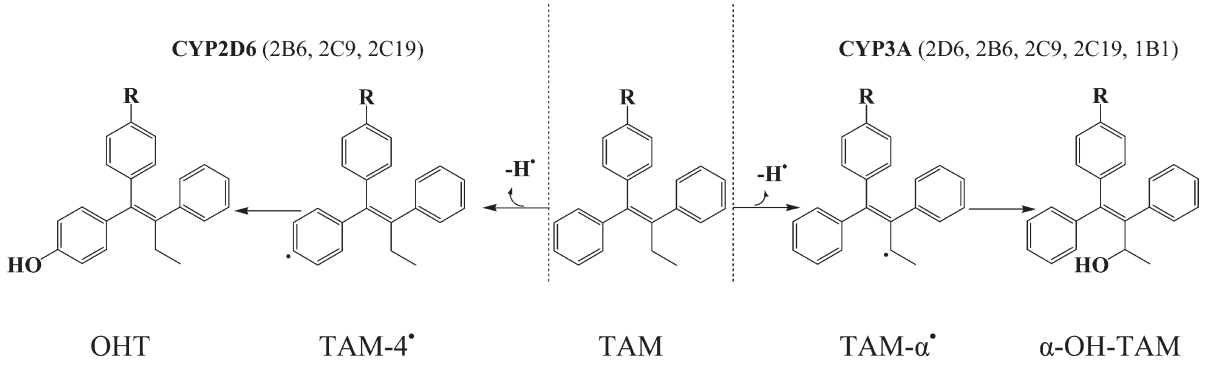

Table 4. Reaction Gibbs Free Energies ($\Delta\Delta G$, in kcal/mol) of the Initial H Atom Abstraction To Yield CYP-Catalyzed 4-Hydroxylation and α-Hydroxylation of TAM and Cis-Trans Isomerization of OHT

reactant	products	ε = 1	ε = 4.24
TAM	TAM-4$^\bullet$ + H$^\bullet$	103.5	103.7
TAM	TAM-$\alpha^\bullet$ + H$^\bullet$	73.7	73.8
OHT-*trans*-**a**	OHT-*trans*-**c**$^\bullet$ + H$^\bullet$	78.1	77.7
OHT-*cis*-**a**	OHT-*cis*-**c**$^\bullet$ + H$^\bullet$	76.8	76.5

for the cationic intermediates (*trans*-/*cis*-**d**$^+$). The C4−O4 bond length decreases from 1.36 Å to 1.22 Å, showing that the quinone moiety C(=O) is the dominant form, and the increased bond length of the central C7−C8 alkene bond from 1.35 Å to 1.43 Å indicates a reduced energy barrier to break the π bond during the rotation. Moreover, the substituents are highly twisted from the plane of the double bond as shown in Figure 1; the dihedral angle 1′−7−8−1″ changes for example from −9.8° (*trans*-**a**) to −21.5° (*trans*-**d**$^+$), which also facilitates the subsequent rotation.

3.3. Rotational Barriers. The rotational barriers about the alkene bond thus obtained are shown in Table 2 for both radical and cationic intermediates. The transition states correspond to the isomerization processes from trans-to-cis′ and cis-to-trans′, with selected geometrical parameters for OHT shown in Table 3.

For the radical pathway, the trans-to-cis or cis-to-trans isomerizations have similar energy barriers, 15−18 kcal/mol. The barriers are much higher than for the cationic pathway and are not significantly reduced by the hydrophobic environment. Furthermore, in the CYP active site, radical lifetimes are generally too short for the subsequent rotational processes of the cis−trans isomerization. Lifetimes of 80−200 fs have been determined experimentally for the radical intermediates of CYP-catalyzed hydroxylation,[45,46] formed by the same initial H abstraction step as the isomerization studied in this work.

The cationic pathway appears to be greatly favored, giving low energy barriers in the gas phase, ∼5.0 kcal/mol for trans-to-cis and ∼10.8 kcal/mol for cis-to-trans, and even lower barriers in a hydrophobic environment. The rotational barriers for trans-to-cis are lower than that for cis-to-trans, mainly because the cis cationic intermediate (*cis*-**d**$^+$) is energetically favored, although the slight energy difference between the [*trans*-**d**$^+$]‡ and [*cis*-**d**$^+$]‡ structures also contributes. In addition, the order of the barriers

Table 5. Ionization Potentials and Deprotonation Energies of the Oxidation Processes as Shown in Scheme 3, for *trans*- and *cis*-OHT/ENDO[a] ($\Delta\Delta G$, in kcal/mol)

		OHT		ENDO	
reactant	products[b]	ε = 1	ε = 4.24	ε = 1	ε = 4.24
trans-**a**	*trans*-**b**$^{+\bullet}$ + e$^-$	158.6	132.8	158.4	133.0
trans-**b**$^{+\bullet}$	*trans*-**c**$^\bullet$ + H$^+$	237.8	263.1	237.9	262.5
trans-**c**$^\bullet$	*trans*-**d**$^+$ + e$^-$	164.1	134.0	164.2	134.3
cis-**a**	*cis*-**b**$^{+\bullet}$ + e$^-$	158.7	132.7	158.7	132.8
cis-**b**$^{+\bullet}$	*cis*-**c**$^\bullet$ + H$^+$	236.5	262.0	236.3	261.8
cis-**c**$^\bullet$	*cis*-**d**$^+$ + e$^-$	161.6	132.2	162.5	132.1

[a] All values are relative to the free energies of the corresponding reaction intermediates. [b] Energy of free H$^+$/e$^-$ are not included on the product side.

between trans-to-cis and cis-to-trans processes is in good agreement with the experimental conversion difference.[22] The data in Table 2 thus implies that the rotations about the alkene bond proceed after the second electron abstraction from the substrate by the ferryl species (i.e., the cationic pathway).

3.4. Computed Isomerization Potentials for the Cationic Pathway. Detailed studies were performed on the isomerization process of OHT via the cationic intermediate. The reaction coordinate is for the conversion between the *trans*-**d**$^+$ and *cis*′-**d**$^+$ isomers defined by the dihedral angle 1′−7−8−1″. The potential energy diagrams shown in Figure 2 were calculated at different fixed values of 1′−7−8−1″ dihedral angle in gas phase (ε = 1) and solvent (ε = 4.24). The DFT model studies provide mechanistic insight on the rotation of a free cationic intermediate. Exploring the processes in nonpolar solvent (ε = 4.24) enables assessment of the barrier heights within a "bulk" hydrophobic protein environment, in which the conversion is found to be easier than in gas phase. The *cis*′-**d**$^+$ conformer is energetically favored, resulting in an easier conversion from trans-to-cis than cis-to-trans and in excellent agreement with experiments.[22] We emphasize, however, that no explicit protein active site was included. This may on the one hand be a shortcoming of the current study; on the other hand many of the CYP active site cavities, in particular for CYPs found in the liver, are very large in order for the enzymes to be able to degrade a wide range of different substrates and xenobiotics.

dx.doi.org/10.1021/ci2001082 |J. Chem. Inf. Model. 2011, 51, 2293–2301

Scheme 5. Possible Mechanism for Dehydrogenation of (1) 4-Hydroxyacetanilide to Iminoquinone and (2) Raloxifene to Diquinone Methide[a] Catalyzed by CYP

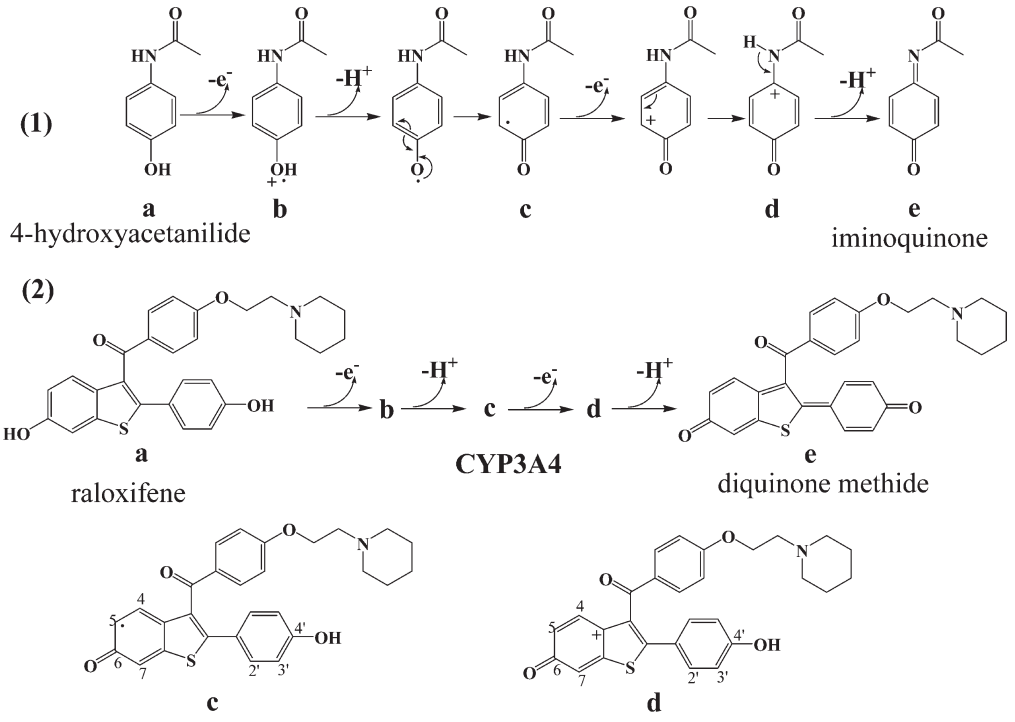

[a] An early study[54] suggested that the dehydrogenation of raloxifene was initiated from the 6-hydroxy group catalyzed by CYP3A4.

3.5. Initial H Atom Abstraction. There has been considerable theoretical work on the initial H atom abstraction of a range of different substrates (although not including TAM and its derivatives) with explicit focus on the oxidation steps in heme-containing CYPs. The generally high activation energy for the H atom abstraction has been shown to be accessible under physiological conditions, due to the highly reactive ferryl species.[47−49] For different target products from TAM and OHT, H atom abstraction is herein assumed to be the initial step for all the three reactions, 4-hydroxylation and α-hydroxylation of TAM (Scheme 4), and cis−trans isomerization of OHT.

The computed reaction energies for H atom abstraction from TAM or OHT are shown in Table 4. The highest reaction energy, ~104 kcal/mol, is required for the abstraction of the 4-H from the aromatic ring of TAM to eventually produce OHT. This aromatic H-abstraction is 30 kcal/mol more endergonic than H-abstraction for the aliphatic α-hydroxylation reaction. The results indicate that the mechanism of CYP-mediated aromatic hydroxylation may differ from the aliphatic hydroxylation route. This is consistent with de Visser's work,[39] showing that an efficient mechanism for aromatic hydroxylation may be initiated via an electrophilic attack of the π system of the aromatic ring, rather than H atom abstraction, and lead to a Fe−O−Ph intermediate, followed by a proton-shuttle.

Because the isomerization does not occur for the nonhydroxylated TAM, a reasonable initial step is H atom abstraction from the 4-hydroxy group. The reaction energy (~77 kcal/mol) is similar to the energy for α-H atom abstraction (~74 kcal/mol). We therefore also propose that the 4-hydroxylation intermediate of TAM, Fe−O−Ph(TAM), does not undergo cis−trans isomerization. Instead the isomerization process of OHT is more likely to proceed via a free cationic intermediate. The cis−trans isomerization and α-hydroxylation are thus most likely to proceed via the same initial step. Experimental results have shown that the recombinant human CYP isoforms which catalyze the cis−trans isomerization also catalyze α-hydroxylation. CYP2B6 and CYP2C19 catalyze all three reactions, whereas CYP1B1, which displayed the highest activity for the isomerization, did not show any additional 4-hydroxylation activity, only α-hydroxylation.[3,50,51]

Table 6. Ionization Potentials and Deprotonation Energies of the Oxidation Processes as Shown in Scheme 5[a] ($\Delta\Delta G$, in kcal/mol)

		4-hydroxyacetanilide		raloxifene[c]	
reactant	products[b]	ε = 1	ε = 4.24	ε = 1	ε = 4.24
a	$\mathbf{b}^{+\bullet} + e^-$	175.1	138.5	158.6	133.3
$\mathbf{b}^{+\bullet}$	$\mathbf{c}^{\bullet} + H^+$	219.5	254.5	236.0	261.1
$\mathbf{c}^{\bullet}$	$\mathbf{d}^{+} + e^-$	174.0	134.6	155.6	127.9
$\mathbf{d}^{+}$	$\mathbf{e} + H^+$	208.8	249.9	234.0	262.6

[a] All values are relative to the free energies of the corresponding reaction intermediates. [b] Energy of free H^+/e^- is not included on the product side. [c] Geometry optimizations and frequency calculations were performed at M06−2X/6-31G(d,p) level of theory.

3.6. The Second Electron Abstraction. The highly oxidative ferryl species is the essential driving force in CYP oxidations and abstracts H atoms or electrons. Because the reactive nature of the ferryl species is electrophilic attack, we propose that the initial H abstraction could be considered as a stepwise electron and proton transfer. Conversely, a sequential electron and proton transfer may differ from the loss of a H atom, because there could in principle be different receptors for the electron and proton. To

verify the abstraction of the second electron being accessible, the ionization potentials and deprotonation energies were computed at the same level of theory as the rotational processes. The results are shown in Table 5. The computed ionization potentials are quite similar for the abstraction of the first and second electron from either trans or cis isomers of OHT/ENDO, which indicates a high probability of the second electron abstraction. The energies required to remove an electron or a proton from the cis vs the trans isomer are highly similar. Therefore, the experimentally observed difference in the cis−trans interconversion is more likely due to the subsequent rotation about the alkene bond than to the oxidation process itself. The redox potentials in conjunction with the rotational barriers support the cationic pathway. The rotational barriers play important roles for the accumulation of cis isomers in vivo, although it may not be the rate-determining step.

The ionization potentials are dramatically affected by the environment and decrease by ∼25 kcal/mol when introducing the dielectric medium of low dielectric constant (ε = 4.24). On the other hand, the subsequent H^+ abstractions are more difficult, by essentially the same amount. The thermochemistry of ionization and deprotonation studied herein cannot provide energy barriers of the oxidation processes for the substrate in complex with the heme unit within the protein active site. Comparison can however be made to the desaturation of 4-hydroxyacetanilide to iminoquinone and raloxifene to diquinone methide (Scheme 5 and Table 6). The dehydrogenation process of 4-hydroxyacetanilide is determined experimentally as a CYP-catalyzed reaction,[52] albeit it is not clear whether this involves hydrogen atom abstractions (Scheme S1 and Table S2 in Supporting Information) or stepwise electron and proton transfer. Raloxifene diquinone methide is also shown experimentally to be directly produced by CYP3A4 from raloxifene itself.[53]

The three reactions are comparable CYP-mediated redox processes on the same type of reactive phenol moiety. As the energies required to remove electrons from 4-hydroxyacetanilide are even higher than for OHT/ENDO, the redox potential of the ferryl species must be high enough to remove electrons from the TAM-based substrates. In the case of 4-hydroxyacetanilide, however, there is a second proton to abstract, giving the desaturated C═N bond. In the case of raloxifene, the energies required for electron and proton abstraction closely mirrors the energies of the redox process of OHT. However, in contrast to the case of OHT, the 4′-hydroxy group of raloxifene provides the second proton available for abstraction, which results in a diquinone methide dehydrogenation product. As this proton is lacking in the TAM derivatives, an unstable cationic intermediate ($\mathbf{d}^+$) is instead formed, followed by isomerization due to the low rotational barrier.

4. CONCLUSIONS

We herein present the results of DFT studies on the mechanism of CYP-catalyzed cis−trans isomerization of the active derivatives OHT and ENDO of anticancer compound TAM. The data strongly suggests that isomerization occurs via a cationic intermediate. The cationic cis-isomer is more than 3 kcal/mol energetically favored than the trans form, resulting in an easier conversion from trans-to-cis than from cis-to-trans, in excellent agreement with experimental data.

The substrate-based DFT studies indicate that the isomerization is initiated by H atom abstraction from the 4-hydroxy group. Because of the lack of a second abstractable H-atom from the ethenyl group of the OHT/ENDO substrates, only a second electron is abstracted. Hence, a CYP-catalyzed desaturation cannot complete to a stable dehydrogenation product, leading instead to the cationic intermediate being formed. The ethylenic double bond of the cationic intermediate is twisted more than for the corresponding neutral/radical species (Figure 1 and Table 1), and thus the energy cost of the rotation about the alkene bond is less expensive and allows for the isomerization to occur. The isomerization process is completed by reversing the hydrogen and electron transfer from the protein environment. The chemical nature of the substrate for analogous CYP-mediated oxidation processes on OHT/ENDO or 4-hydroxyacetanilide/raloxifene results in distinctly different reactions, i.e., isomerization vs dehydrogenation, respectively.

Substrate-based studies of the CYP-catalyzed reactions are reported, including cis−trans isomerization of OHT, 4- and α-hydroxylation of TAM, and dehydrogenation of 4-hydroxyacetanilide/raloxifene to quinone-like products. The results indicate related mechanisms for these reactions except for the aromatic hydroxylation and show that the CYP reactions also depend on the chemical nature of the substrates, besides the CYP active site.

■ ASSOCIATED CONTENT

Supporting Information. Computational details, additional computational data, a list of total energies for all species and Cartesian coordinates of the transition states discussed herein. This material is available free of charge via the Internet at http://pubs.acs.org.

■ AUTHOR INFORMATION

Corresponding Author

*Phone: +353-91-492450. Fax: +353-91-525700. E-mail: leif.eriksson@nuigalway.ie.

Present Addresses

[⊥]Department of Theoretical Chemistry and Biology, School of Biotechnology, Royal Institute of Technology, S-106 91 Stockholm, Sweden.

[∥]Department of Chemistry, University of Gothenburg, 412 96 Göteborg, Sweden.

■ ACKNOWLEDGMENT

We are grateful for financial support from the Faculty of Science and Technology at Örebro University and the National University of Ireland, Galway.

■ REFERENCES

(1) Jordan, V. C. Tamoxifen: A most unlikely pioneering medicine. *Nat. Rev. Drug Discovery* **2003**, *2*, 205–213.

(2) Jin, Y.; Desta, Z.; Stearns, V.; Ward, B.; Ho, H.; Lee, K. H.; Skaar, T.; Storniolo, A. M.; Li, L.; Araba, A.; Blanchard, R.; Nguyen, A.; Ullmer, L.; Hayden, J.; Lemler, S.; Weinshilboum, R. M.; Rae, J. M.; Hayes, D. F.; Flockhart, D. A. CYP2D6 genotype, antidepressant use, and tamoxifen metabolism during adjuvant breast cancer treatment. *J. Natl. Cancer Inst.* **2005**, *97*, 30–39.

(3) Desta, Z.; Ward, B. A.; Soukhova, N. V.; Flockhart, D. A. Comprehensive evaluation of tamoxifen sequential biotransformation by the human cytochrome P450 system in vitro: Prominent roles for CYP3A and CYP2D6. *J. Pharmacol. Exp. Ther.* **2004**, *310*, 1062–1075.

(4) Potter, G. A.; Mccague, R.; Jarman, M. A Mechanistic Hypothesis for DNA Adduct Formation by Tamoxifen Following Hepatic Oxidative-Metabolism. *Carcinogenesis* **1994**, *15*, 439–442.

(5) Fabian, C.; Tilzer, L.; Sternson, L. Comparative Binding Affinities of Tamoxifen, 4-Hydroxytamoxifen, and Desmethyltamoxifen for Estrogen-Receptors Isolated from Human-Breast Carcinoma - Correlation with Blood-Levels in Patients with Metastatic Breast-Cancer. *Biopharm. Drug Dispos.* **1981**, *2*, 381–390.

(6) Johnson, M. D.; Zuo, H.; Lee, K. H.; Trebley, J. P.; Rae, J. M.; Weatherman, R. V.; Desta, Z.; Flockhart, D. A.; Skaar, T. C. Pharmacological characterization of 4-hydroxy-*N*-desmethyl tamoxifen, a novel active metabolite of tamoxifen. *Breast Cancer Res. Treat.* **2004**, *85*, 151–159.

(7) Coezy, E.; Borgna, J. L.; Rochefort, H. Tamoxifen and Metabolites in Mcf7 Cells - Correlation between Binding to Estrogen-Receptor and Inhibition of Cell-Growth. *Cancer Res.* **1982**, *42*, 317–323.

(8) Kaftory, M.; Biali, S. E.; Rappoport, Z. Stable Simple Enols. 9. Solid-State Structures and Conformations of Several Simple Enols and Their Keto Tautomers. *J. Am. Chem. Soc.* **1985**, *107*, 1701–1709.

(9) Biali, S. E.; Rappoport, Z. Stable Simple Enols. 3. Static and Dynamic Nmr Behavior of Crowded Triarylethenols and Related-Compounds - 3-Ring Flip as the Threshold Mechanism for Enantiomerization of Crowded Triarylvinyl Propellers. *J. Am. Chem. Soc.* **1984**, *106*, 477–496.

(10) Precigoux, G.; Courseille, C.; Geoffre, S.; Hospital, M. [p-(Dimethylamino-2 -ethoxy)phenyl]-1-trans-diphenyl-1,2-butene-1-(Tamoxifen)(ICI-46474). *Acta Crystallogr., Sect. B: Struct. Sci.* **1979**, *35*, 3070–3072.

(11) Shiau, A. K.; Barstad, D.; Loria, P. M.; Cheng, L.; Kushner, P. J.; Agard, D. A.; Greene, G. L. The structural basis of estrogen receptor/coactivator recognition and the antagonism of this interaction by tamoxifen. *Cell* **1998**, *95*, 927–937.

(12) Heldring, N.; Pawson, T.; McDonnell, D.; Treuter, E.; Gustafsson, J. A.; Pike, A. C. Structural insights into corepressor recognition by antagonist-bound estrogen receptors. *J. Biol. Chem.* **2007**, *282*, 10449–10455.

(13) Kong, E. H.; Heldring, N.; Gustafsson, J. A.; Treuter, E.; Hubbard, R. E.; Pike, A. C. Delineation of a unique protein-protein interaction site on the surface of the estrogen receptor. *Proc. Natl. Acad. Sci. U.S.A.* **2005**, *102*, 3593–3598.

(14) Rappoport, Z.; Biali, S. E. Threshold rotational mechanisms and enantiomerization barriers of polyarylvinyl propellers. *Acc. Chem. Res.* **1997**, *30*, 307–314.

(15) Kuramochi, H. Conformational studies and electronic structures of tamoxifen and toremifene and their allylic carbocations proposed as reactive intermediates leading to DNA adduct formation. *J. Med. Chem.* **1996**, *39*, 2877–2886.

(16) McCague, R.; Kuroda, R.; Leclercq, G.; Stoessel, S. Synthesis and estrogen receptor binding of 6,7-dihydro-8-phenyl-9-[4-[2-(dimethylamino)ethoxy] phenyl]-5*H*-benzocycloheptene, a nonisomerizable analogue of tamoxifen. X-ray crystallographic studies. *J. Med. Chem.* **1986**, *29*, 2053–2059.

(17) Jordan, V. C.; Koch, R.; Langan, S.; Mccague, R. Ligand Interaction at the Estrogen-Receptor to Program Antiestrogen Action - a Study with Nonsteroidal Compounds Invitro. *Endocrinology* **1988**, *122*, 1449–1454.

(18) Katzenellenbogen, B. S.; Norman, M. J.; Eckert, R. L.; Peltz, S. W.; Mangel, W. F. Bioactivities, Estrogen-Receptor Interactions, and Plasminogen Activator-Inducing Activities of Tamoxifen and Hydroxytamoxifen Isomers in Mcf-7 Human-Breast Cancer-Cells. *Cancer Res.* **1984**, *44*, 112–119.

(19) Osborne, C. K.; Wiebe, V. J.; Mcguire, W. L.; Ciocca, D. R.; Degregorio, M. W. Tamoxifen and the Isomers of 4-Hydroxytamoxifen in Tamoxifen-Resistant Tumors from Breast-Cancer Patients. *J. Clin. Oncol.* **1992**, *10*, 304–310.

(20) Osborne, C. K.; Coronado, E.; Allred, D. C.; Wiebe, V.; Degregorio, M. Acquired Tamoxifen Resistance - Correlation with Reduced Breast-Tumor Levels of Tamoxifen and Isomerization of Trans-4-Hydroxytamoxifen. *J. Natl. Cancer Inst.* **1991**, *83*, 1477–1482.

(21) Lazarus, P.; Blevins-Primeau, A. S.; Zheng, Y.; Sun, D. X. Potential Role of UGT Pharmacogenetics in Cancer Treatment and Prevention Focus on Tamoxifen. *Steroid Enzyme Cancer* **2009**, *1155*, 99–111.

(22) Williams, M. L.; Lennard, M. S.; Martin, I. J.; Tucker, G. T. Interindividual Variation in the Isomerization of 4-Hydroxytamoxifen by Human Liver-Microsomes - Involvement of Cytochromes P450. *Carcinogenesis* **1994**, *15*, 2733–2738.

(23) Crewe, H. K.; Notley, L. M.; Wunsch, R. M.; Lennard, M. S.; Gillam, E. M. J. Metabolism of tamoxifen by recombinant human cytochrome P450 enzymes: Formation of the 4-hydroxy, 4′-hydroxy and *N*-desmethyl metabolites and isomerization of trans-4-hydroxytamoxifen. *Drug Metab. Dispos.* **2002**, *30*, 869–874.

(24) Sono, M.; Roach, M. P.; Coulter, E. D.; Dawson, J. H. Heme-containing oxygenases. *Chem. Rev.* **1996**, *96*, 2841–2887.

(25) Guengerich, F. P. Common and uncommon cytochrome P450 reactions related to metabolism and chemical toxicity. *Chem. Res. Toxicol.* **2001**, *14*, 611–650.

(26) Shaik, S.; Kumar, D.; de Visser, S. P.; Altun, A.; Thiel, W. Theoretical perspective on the structure and mechanism of cytochrome P450 enzymes. *Chem. Rev.* **2005**, *105*, 2279–2328.

(27) Shaik, S.; Cohen, S.; Wang, Y.; Chen, H.; Kumar, D.; Thiel, W. P450 Enzymes: Their Structure, Reactivity, and Selectivity-Modeled by QM/MM Calculations. *Chem. Rev.* **2010**, *110*, 949–1017.

(28) Nussinov, R.; Fishelovitch, D.; Shaik, S.; Wolfson, H. J. How Does the Reductase Help To Regulate the Catalytic Cycle of Cytochrome P450 3A4 Using the Conserved Water Channel? *J. Phys. Chem. B* **2010**, *114*, 5964–5970.

(29) Schyman, P.; Lai, W.; Chen, H.; Wang, Y.; Shaik, S. The directive of the protein: how does cytochrome p450 select the mechanism of dopamine formation? *J. Am. Chem. Soc.* **2011**, *133*, 7977–7984.

(30) Friesner, R. A.; Bochevarov, A. D.; Li, J. N.; Song, W. J.; Lippard, S. Insights into the Different Dioxygen Activation Pathways of Methane and Toluene Monooxygenase Hydroxylases. *J. Am. Chem. Soc.* **2011**, *133*, 7384–7397.

(31) Han, K. L.; Li, D. M.; Huang, X. Q.; Zhan, C. G. Catalytic Mechanism of Cytochrome P450 for 5′-Hydroxylation of Nicotine: Fundamental Reaction Pathways and Stereoselectivity. *J. Am. Chem. Soc.* **2011**, *133*, 7416–7427.

(32) Guengerich, F. P.; Macdonald, T. L. Chemical Mechanisms of Catalysis by Cytochromes-P-450 - a Unified View. *Acc. Chem. Res.* **1984**, *17*, 9–16.

(33) Meunier, B.; de Visser, S. P.; Shaik, S. Mechanism of oxidation reactions catalyzed by cytochrome P450 enzymes. *Chem. Rev.* **2004**, *104*, 3947–3980.

(34) Groves, J. T.; Mcclusky, G. A. Aliphatic Hydroxylation Via Oxygen Rebound - Oxygen-Transfer Catalyzed by Iron. *J. Am. Chem. Soc.* **1976**, *98*, 859–861.

(35) Groves, J. T. Key Elements of the Chemistry of Cytochrome-P-450 - the Oxygen Rebound Mechanism. *J. Chem. Educ.* **1985**, *62*, 928–931.

(36) Wand, M. D.; Thompson, J. A. Cytochrome-P-450-Catalyzed Rearrangement of a Peroxyquinol Derived from Butylated Hydroxytoluene - Involvement of Radical and Cationic Intermediates. *J. Biol. Chem.* **1986**, *261*, 14049–14056.

(37) Kumar, D.; De Visser, S. P.; Shaik, S. Oxygen economy of cytochrome P450: what is the origin of the mixed functionality as a dehydrogenase-oxidase enzyme compared with its normal function? *J. Am. Chem. Soc.* **2004**, *126*, 5072–5073.

(38) Macdonald, T. L.; Gutheim, W. G.; Martin, R. B.; Guengerich, F. P. Oxidation of Substituted *N*,*N*-Dimethylanilines by Cytochrome-P-450 - Estimation of the Effective Oxidation Reduction Potential of Cytochrome-P-450. *Biochemistry* **1989**, *28*, 2071–2077.

(39) de Visser, S. P.; Shaik, S. A proton-shuttle mechanism mediated by the porphyrin in benzene hydroxylation by cytochrome P450 enzymes. *J. Am. Chem. Soc.* **2003**, *125*, 7413–7424.

(40) Bach, R. D. The rate-limiting step in P450 hydroxylation of hydrocarbons a direct comparison of the "somersault" versus the

"consensus" mechanism involving compound I. *J. Phys. Chem. A* **2010**, *114*, 9319–9332.

(41) Zhao, Y.; Truhlar, D. G. The M06 suite of density functionals for main group thermochemistry, thermochemical kinetics, noncovalent interactions, excited states, and transition elements: two new functionals and systematic testing of four M06-class functionals and 12 other functionals. *Theor. Chem. Acc.* **2008**, *120*, 215–241.

(42) Zhao, Y.; Truhlar, D. G. Density functionals with broad applicability in chemistry. *Acc. Chem. Res.* **2008**, *41*, 157–167.

(43) Marenich, A. V.; Cramer, C. J.; Truhlar, D. G. Universal Solvation Model Based on Solute Electron Density and on a Continuum Model of the Solvent Defined by the Bulk Dielectric Constant and Atomic Surface Tensions. *J. Phys. Chem. B* **2009**, *113*, 6378–6396.

(44) Frisch, M. J.; Trucks, G. W.; Schlegel, H. B.; Scuseria, G. E.; Robb, M. A.; Cheeseman, J. R.; Scalmani, G.; Barone, V.; Mennucci, B.; Petersson, G. A.; Nakatsuji, H.; Caricato, M.; Li, X.; Hratchian, H. P.; Izmaylov, A. F.; Bloino, J.; Zheng, G.; Sonnenberg, J. L.; Hada, M.; Ehara, M.; Toyota, K.; Fukuda, R.; Hasegawa, J.; Ishida, M.; Nakajima, T.; Honda, Y.; Kitao, O.; Nakai, H.; Vreven, T.; Montgomery, J. A.; Jr.; Peralta, J. E.; Ogliaro, F.; Bearpark, M.; Heyd, J. J.; Brothers, E.; Kudin, K. N.; Staroverov, V. N.; Kobayashi, R.; Normand, J.; Raghavachari, K.; Rendell, A.; Burant, J. C.; Iyengar, S. S.; Tomasi, J.; Cossi, M.; Rega, N.; Millam, J. M.; Klene, M.; Knox, J. E.; Cross, J. B.; Bakken, V.; Adamo, C.; Jaramillo, J.; Gomperts, R.; Stratmann, R. E.; Yazyev, O.; Austin, A. J.; Cammi, R.; Pomelli, C.; Ochterski, J. W.; Martin, R. L.; Morokuma, K.; Zakrzewski, V. G.; Voth, G. A.; Salvador, P.; Dannenberg, J. J.; Dapprich, S.; Daniels, A. D.; Farkas, O.; Foresman, J. B.; Ortiz, J. V.; Cioslowski, J.; Fox, D. J. *Gaussian 09*; Gaussian, Inc., Wallingford, CT, 2009.

(45) Newcomb, M.; Letadicbiadatti, F. H.; Chestney, D. L.; Roberts, E. S.; Hollenberg, P. F. A Nonsynchronous Concerted Mechanism for Cytochrome-P-450 Catalyzed Hydroxylation. *J. Am. Chem. Soc.* **1995**, *117*, 12085–12091.

(46) Toy, P. H.; Newcomb, M.; Hollenberg, P. F. Hypersensitive mechanistic probe studies of cytochrome P450-catalyzed hydroxylation reactions. Implications for the cationic pathway. *J. Am. Chem. Soc.* **1998**, *120*, 7719–7729.

(47) Kamachi, T.; Yoshizawa, K. A theoretical study on the mechanism of camphor hydroxylation by compound I of cytochrome P450 *J. Am. Chem. Soc.* **2003**, *125*, 4652–4661.

(48) Guallar, V.; Baik, M. H.; Lippard, S. J.; Friesner, R. A. Peripheral heme substituents control the hydrogen-atom abstraction chemistry in cytochromes P450. *Proc. Natl. Acad. Sci. U.S.A.* **2003**, *100*, 6998–7002.

(49) de Visser, S. P.; Ogliaro, F.; Sharma, P. K.; Shaik, S. What factors affect the regioselectivity of oxidation by cytochrome P450? A DFT study of allylic hydroxylation and double bond epoxidation in a model reaction. *J. Am. Chem. Soc.* **2002**, *124*, 11809–11826.

(50) Crewe, H. K.; Notley, L. M.; Wunsch, R. M.; Lennard, M. S.; Gillam, E. M. Metabolism of tamoxifen by recombinant human cytochrome P450 enzymes: formation of the 4-hydroxy, 4′-hydroxy and N-desmethyl metabolites and isomerization of trans-4-hydroxytamoxifen. *Drug Metab. Dispos.* **2002**, *30*, 869–874.

(51) Sharma, M.; Shubert, D. E.; Lewis, J.; McGarrigle, B. P.; Bofinger, D. P.; Olson, J. R. Biotransformation of tamoxifen in a human endometrial explant culture model. *Chem.-Biol. Interact.* **2003**, *146*, 237–249.

(52) Nelson, S. D.; Forte, A. J.; Dahlin, D. C. Lack of Evidence for N-Hydroxyacetaminophen as a Reactive Metabolite of Acetaminophen Invitro. *Biochem. Pharmacol.* **1980**, *29*, 1617–1620.

(53) Yost, G. S.; Moore, C. D.; Reilly, C. A. CYP3A4-Mediated Oxygenation versus Dehydrogenation of Raloxifene. *Biochemistry* **2010**, *49*, 4466–4475.

(54) Yost, G. S.; Moore, C. D.; Shahrokh, K.; Sontum, S. F.; Cheatham, T. E. Improved Cytochrome P450 3A4Molecular Models Accurately Predict the Phe215 Requirement for Raloxifene Dehydrogenation Selectivity. *Biochemistry* **2010**, *49*, 9011–9019.